

DC Motor Drive Design Project

Topology Selection, Simulation, and Component Selection

Group Name/Number

Yunus Tosun (2517084)

Alihan Kale (2516334)

Hüseyin Oğuz (2516623)

December 5, 2025

Contents

1 Topology Selection and Analysis	4
1.1 Design Requirements and Constraints	4
1.2 Candidate Topologies	4
1.2.1 Option A: Single-Phase Rectifier + Buck Converter	4
1.2.2 Option B: Three-Phase Rectifier + Buck Converter	4
1.2.3 Option C: Synchronous Buck (Half-Bridge) Converter	5
1.3 Comparative Analysis Matrix	6
1.4 Final Selection and Justification	6
2 DC Motor Modeling and Verification	7
2.1 Parameter Extraction	7
2.1.1 Field-Armature Mutual Inductance (L_{af})	7
2.1.2 Mechanical Parameters	7
2.2 Model Verification Results	7
3 Computer Simulation and Analysis	9
3.1 Phase I: Topology Selection and Idealized Verification	9
3.2 Phase II: High-Fidelity Hardware Modeling	9
3.2.1 Parameter Extraction	9
3.2.2 Control Logic (Soft Start)	10
3.3 Simulation Results and Physics Analysis	10
3.3.1 1. Startup and Friction Dead-Band (0 – 0.22 s)	11
3.3.2 2. Light-Load Fluctuations (0.22 – 2.5 s)	11
3.3.3 3. Load Step Response ($t = 2.5$ s)	11
3.3.4 Ripple Verification	12
4 Component Selection and Sizing	13
4.1 Power Semiconductor Selection	13
4.1.1 Primary Switch (IGBT)	13
4.1.2 Freewheeling Diode	13
4.1.3 Input Rectifier	13
4.2 Thermal Management Design	13
4.3 Gate Drive and Control Topology	14
4.4 Passive Components	14
A Technical Note: Power Stage Semiconductor Selection	15
A.1 Executive Summary	15
A.2 System Requirements	15
A.3 Component Analysis: Option A (MOSFET)	15
A.3.1 Current Rating Violation	15
A.3.2 Thermal Analysis (Power Loss)	15
A.4 Component Analysis: Option B (IGBT)	16
A.4.1 Suitability and Thermal Analysis	16
A.5 Implementation Details	16
A.5.1 Gate Drive Strategy	16
A.5.2 Final Recommendation	16

List of Figures

1	Proposed Topology: Three-Phase Diode Rectifier with Buck Converter	5
2	Motor Step Response: Speed (top) and Armature Current (bottom). A rated load torque of 26.1 Nm is applied at t=2s, causing the speed to settle near the rated 1500 RPM.	8
3	Overview of the High-Fidelity Simulink model showing the Parametrized Rectifier, Buck Converter with real switch models, and the Coupled Motor-Generator Set.	9
4	High-Fidelity Simulation Results. Top: Motor Speed. Bottom: Armature Current. Note the distinct phases of friction breakaway, acceleration, and load impact.	11
5	Armature Current Ripple Analysis. The simulation confirms $f_{sw} = 10$ kHz.	12
6	Steady-state dissipated MOSFET power vs. time.	16

List of Tables

1	Topology Comparison Matrix	6
2	Derived Simulation Parameters for DC Machine	7
3	Simulation Parameters: Ideal vs. Datasheet-Derived	10

1 Topology Selection and Analysis

1.1 Design Requirements and Constraints

The primary objective of this project is to design a DC motor drive capable of providing a controllable output voltage (V_{out}) up to 180 V. The critical constraint defining the topology selection is the output current ripple frequency requirement:

$$f_{ripple} > 1 \text{ kHz} \quad (1)$$

Standard line-commutated converters (such as controlled thyristor bridges) produce ripple frequencies dependent on the grid frequency ($2f_{grid} = 100 \text{ Hz}$ for single-phase, $6f_{grid} = 300 \text{ Hz}$ for three-phase). To meet the $> 1 \text{ kHz}$ requirement, a Switch Mode Power Supply (SMPS) approach—specifically a DC-DC chopper—is required. Therefore, all topologies considered utilize a two-stage conversion process:

1. **AC-DC Rectification:** Uncontrolled diode rectification to create a DC bus.
2. **DC-DC Conversion:** High-frequency switching to control the motor voltage and satisfy the ripple frequency constraint.

1.2 Candidate Topologies

Three primary topologies were evaluated for this application.

1.2.1 Option A: Single-Phase Rectifier + Buck Converter

This topology utilizes a single-phase AC input rectified by a full-bridge diode rectifier, followed by a standard step-down (buck) converter.

- **Advantages:**
 - Simplest implementation and lowest component count.
 - Easier PCB/Stripboard layout due to fewer power traces.
- **Disadvantages:**
 - **High DC Link Ripple:** The rectified voltage drops to zero every half-cycle (without capacitance). To maintain a stable DC link voltage above the required motor voltage (180 V), a very large and physically bulky DC-link capacitor is required.
 - **High Current Stress:** The single-phase input diodes must handle the full power load, increasing thermal management requirements.

1.2.2 Option B: Three-Phase Rectifier + Buck Converter

This topology utilizes a three-phase AC input rectified by a 6-pulse diode bridge, creating a DC link that feeds the buck converter (see Figure 1).

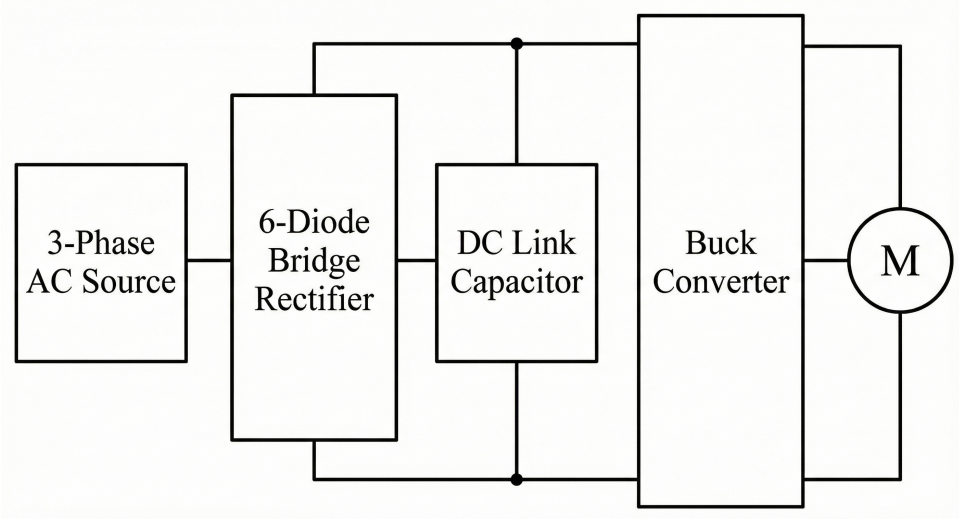


Figure 1: Proposed Topology: Three-Phase Diode Rectifier with Buck Converter

- **Advantages:**

- **Superior DC Link Quality:** The voltage ripple of a 3-phase rectifier is significantly lower (approx. 4%) and the frequency is higher (300 Hz). The voltage never drops to zero (minimum $\approx 1.5 \times V_{line-peak}$).
- **Reduced Capacitor Requirements:** Due to the smoother rectified voltage, the DC link capacitor can be smaller while still maintaining the “headroom” voltage required for the buck converter operation.
- **Load Balancing:** Draws power symmetrically from the grid, which is standard industrial practice.

- **Disadvantages:**

- Requires a 3-phase source (available per project specs) and 6 diodes.
- Slightly more complex input wiring.

1.2.3 Option C: Synchronous Buck (Half-Bridge) Converter

This topology replaces the freewheeling diode of the standard Buck converter with a second MOSFET/IGBT.

- **Advantages:**

- **Regenerative Braking:** Allows current to flow from the motor back to the DC link, enabling active braking.
- **Efficiency:** Lower conduction losses in the low-side switch compared to a diode.

- **Disadvantages:**

- **Shoot-Through Risk:** Requires precise “dead-time” control to prevent shorting the DC link.

- **Drive Complexity:** Requires a complex gate driver with bootstrap circuitry. Given the project timeline and the “Safe Stop” requirement (which can be achieved by coasting), this adds unnecessary risk.

1.3 Comparative Analysis Matrix

Table 1: Topology Comparison Matrix

Feature	1-Phase + Buck	3-Phase + Buck	Sync Buck
Complexity	Low	Low-Medium	High
DC Link Stability	Low	High	High
Capacitor Stress	High	Low	Low
Ripple Frequency	> 1 kHz	> 1 kHz	> 1 kHz
Risk Factor	Medium (Voltage Sag)	Low	High (Control Logic)

1.4 Final Selection and Justification

Based on the analysis above and the comparison in Table 1, the team has selected **Option B: Three-Phase Diode Rectifier + Buck Converter.**

Justification 1: Voltage Headroom The motor requires a maximum voltage ($V_{out,max}$) of 180 V. A buck converter can only step down voltage ($V_{out} = D \times V_{in}$). Therefore, the DC link voltage (V_{in}) must consistently remain above 180 V plus the voltage drops across switches and inductors.

$$V_{link,min} > \frac{V_{out,max}}{D_{max}} \approx \frac{180 \text{ V}}{0.95} \approx 190 \text{ V} \quad (2)$$

A 3-phase rectifier provides a stiff DC voltage averaging $1.35 \times V_{LL}$. Using the Variac to provide a line-to-line voltage of approx 150 V_{rms} will result in a DC link of ≈ 200 V, providing the necessary headroom with minimal capacitance. A single-phase rectifier would require excessive capacitance to prevent the DC link from dipping below 190 V in the valleys of the AC sine wave.

Justification 2: Reliability and Timeline The 3-phase diode bridge is extremely robust and minimizes stress on the DC link capacitor, which is a common failure point. The standard Buck topology (single switch) eliminates the risk of “shoot-through” associated with half-bridge topologies, simplifying the gate drive requirements to a single isolated driver. This aligns with the project goal of reaching a robust, working prototype by the demo deadline.

Justification 3: Ripple Requirement By selecting a switching frequency (f_{sw}) for the Buck converter in the range of 5 kHz – 20 kHz, we inherently satisfy the project requirement of $f_{ripple} > 1$ kHz.

2 DC Motor Modeling and Verification

Before designing the power electronics converter, the DC motor parameters were calculated and verified in the Simulink environment to ensure the simulation model accurately represents the physical plant.

2.1 Parameter Extraction

The available motor is a 5.5 HP, 220 V, 1500 RPM Separately Excited DC Machine. While the electrical resistances (R_a, R_f) and inductances (L_a, L_f) were measured directly, the mechanical and electromagnetic parameters required for the Simulink “DC Machine” block were derived analytically.

2.1.1 Field-Armature Mutual Inductance (L_{af})

The mutual inductance determines the back-EMF generated for a given field current. Using the rated values ($V_t = 220$ V, $I_a = 23.4$ A, $\omega = 157$ rad/s) and the measured total armature resistance ($R_{total} = 0.8 + 0.27 = 1.07$ Ω):

$$E_a = V_t - I_a R_{total} = 220 - (23.4 \times 1.07) \approx 195 \text{ V} \quad (3)$$

With a field current $I_f \approx 1.05$ A (at 220 V excitation), L_{af} was calculated as:

$$L_{af} = \frac{E_a}{I_f \cdot \omega} = \frac{195}{1.05 \cdot 157} \approx 1.18 \text{ H} \quad (4)$$

2.1.2 Mechanical Parameters

To account for the coupled generator setup, the total inertia (J) was estimated to be double that of a standard motor ($0.06 \text{ kg} \cdot \text{m}^2$). The viscous friction coefficient (B_m) was derived assuming friction losses are approximately 2% of the rated power.

The final parameters used in the simulation are summarized in Table 2.

Table 2: Derived Simulation Parameters for DC Machine

Parameter	Symbol	Value
Armature Resistance	R_a	1.07Ω
Armature Inductance	L_a	24.5 mH
Field Resistance	R_f	210Ω
Mutual Inductance	L_{af}	1.18 H
Total Inertia	J	$0.06 \text{ kg} \cdot \text{m}^2$
Viscous Friction	B_m	$0.0032 \text{ N} \cdot \text{m} \cdot \text{s}$

2.2 Model Verification Results

A test simulation was conducted to verify these parameters. The motor was supplied with rated voltage (220 V DC) and subjected to a step load torque of 26.1 Nm (Rated Torque) at $t = 2.0$ s. The resulting transient response is visualized in Figure 2.

- **No-Load Condition ($t < 2$ s):** The motor speed settles at approximately 177 rad/s (1690 RPM).
- **Full-Load Condition ($t > 2$ s):** Upon application of rated torque, the speed drops to 159 rad/s (1518 RPM) and the current settles at 21 A.

These results deviate by less than 1.5% from the nameplate speed of 1500 RPM, confirming that the dynamic model is accurate enough for drive design.

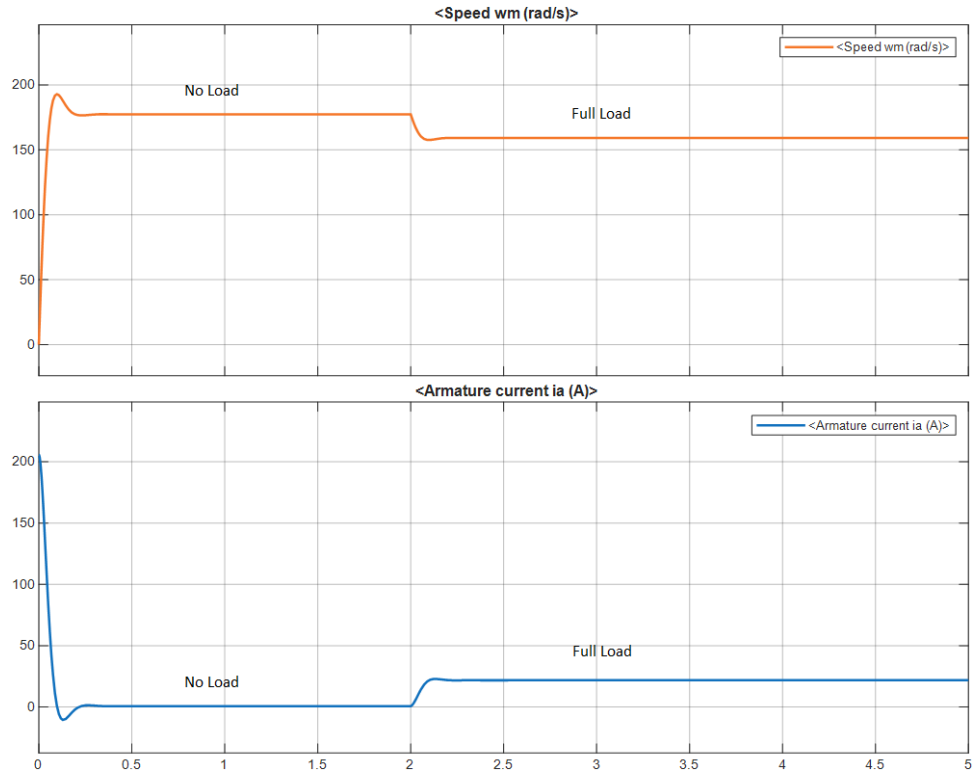


Figure 2: Motor Step Response: Speed (top) and Armature Current (bottom). A rated load torque of 26.1 Nm is applied at $t=2$ s, causing the speed to settle near the rated 1500 RPM.

3 Computer Simulation and Analysis

To ensure a robust design that meets the project deadlines and safety requirements, the simulation process was conducted in two distinct phases. **Phase I** utilized ideal components to verify the topology and control logic. **Phase II** introduced non-linear physical parameters extracted from component datasheets to predict thermal stresses, voltage drops, and transient behavior in the actual laboratory environment.

3.1 Phase I: Topology Selection and Idealized Verification

Initial simulations were conducted using ideal switches and lossless passive components to validate the fundamental operation of the Three-Phase Rectifier + Buck Converter topology.

- **Objective:** Verify that a 10 kHz switching frequency yields the required current ripple ($> 1 \text{ kHz}$) and that the DC link voltage remains sufficiently above 180 V.
- **Outcome:** The topology was confirmed capable of driving the motor. However, the ideal models exhibited perfectly smooth DC voltages and 100% efficiency, failing to account for component voltage drops (diode V_f , IGBT V_{ce}) and capacitor ESR. Consequently, a more detailed model was required to accurately dimension the hardware components.

3.2 Phase II: High-Fidelity Hardware Modeling

In the second phase, the Simulink model was upgraded to represent the "Digital Twin" of the physical prototype. Figure 3 illustrates the system architecture.

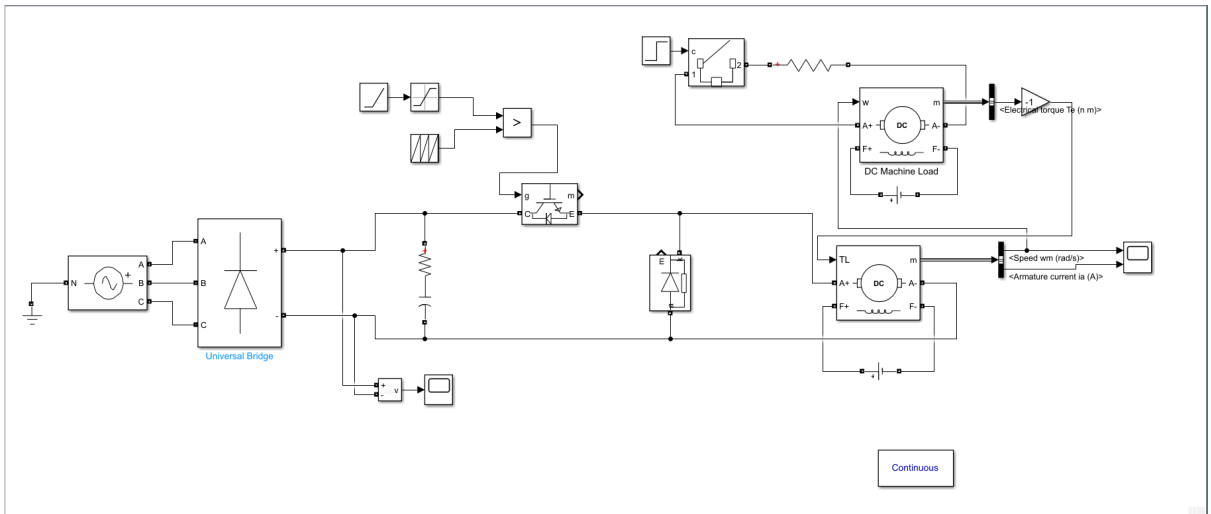


Figure 3: Overview of the High-Fidelity Simulink model showing the Parametrized Rectifier, Buck Converter with real switch models, and the Coupled Motor-Generator Set.

3.2.1 Parameter Extraction

The parameters for the power stage were derived directly from the datasheets of the selected inventory components (IXGH24N60C4D1 IGBT, MUR1560 Diodes, and SQL3510 Rectifier). Table 3 summarizes the transition from ideal to physical parameters.

Table 3: Simulation Parameters: Ideal vs. Datasheet-Derived

Component	Parameter	Ideal Model	High-Fidelity Model
IGBT Switch (IXGH24N60)	R_{on}	0.001 Ω	0.042 Ω
	$V_{CE(sat)}$	0.0 V	1.2 V (Threshold)
Freewheeling Diode (2x MUR1560 Parallel)	R_{on}	0.001 Ω	0.028 Ω
	V_f	0.0 V	0.85 V
Input Rectifier (SQL3510 / Generic)	V_f	0.0 V	0.8 V
	R_{on}	0.001 Ω	0.01 Ω
DC Link Capacitor (470 μF , 400 V)	ESR Type	0 Ω Ideal C	0.68 Ω Series R-C Branch

By incorporating Equivalent Series Resistance (ESR) and semiconductor voltage drops, the simulation accurately predicts the "System Efficiency" and the realistic ripple voltage on the DC bus.

3.2.2 Control Logic (Soft Start)

To protect the hardware from potential inrush currents and mechanical stress, an Open-Loop Soft Start mechanism was implemented. A ramp function increases the duty cycle linearly from 0% to 85% over 2.0 seconds.

$$D(t) = \begin{cases} 0 & t < 0 \\ 0.425 \cdot t & 0 \leq t \leq 2.0 \\ 0.85 & t > 2.0 \end{cases} \quad (5)$$

3.3 Simulation Results and Physics Analysis

The high-fidelity simulation was executed for 4.0 seconds to observe the complete startup and load acceptance cycle. The resulting waveforms (Figure 4) reveal three distinct physical modes of operation.

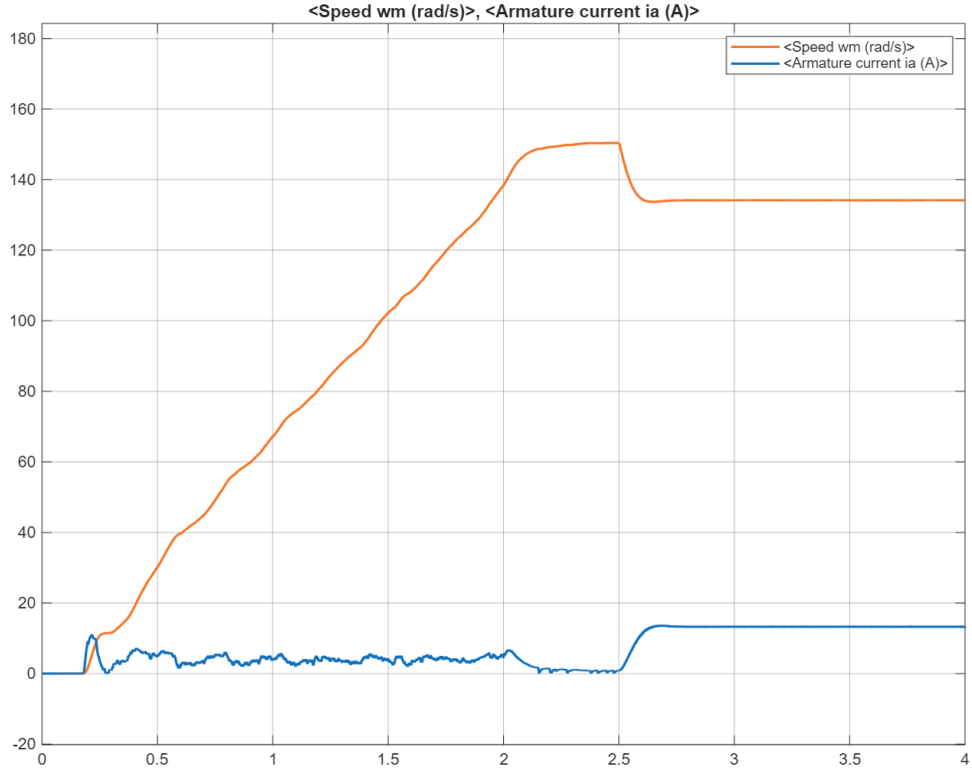


Figure 4: High-Fidelity Simulation Results. Top: Motor Speed. Bottom: Armature Current. Note the distinct phases of friction breakaway, acceleration, and load impact.

3.3.1 1. Startup and Friction Dead-Band (0 – 0.22 s)

The motor does not rotate immediately. This is a correct physical representation of **Stiction** (Coulomb Friction). The Soft Start initially applies a very low duty cycle (< 10%). The resulting current is insufficient to overcome the static friction torque ($T_f = 0.3 \text{ Nm}$). Motion begins only at $t = 0.22 \text{ s}$ when the electromagnetic torque exceeds stiction.

3.3.2 2. Light-Load Fluctuations (0.22 – 2.5 s)

During acceleration under no-load conditions, minor oscillations are observed in the speed and current waveforms. This is identified as **Discontinuous Conduction Mode (DCM)**.

- Because the average current required to spin the unloaded motor is very low (< 1 A), the inductor current falls to zero during the "OFF" period of the switching cycle.
- Additionally, the 300 Hz voltage ripple from the rectifier creates a beat frequency that modulates the motor current.

These fluctuations are normal for a buck converter operating at light loads and do not indicate instability.

3.3.3 3. Load Step Response ($t = 2.5 \text{ s}$)

At $t = 2.5 \text{ s}$, the generator breaker closes, applying the full resistive load.

- **Transient:** The speed momentarily dips as the generator produces braking torque.
- **Recovery:** The system naturally stabilizes. The armature current rises sharply to the rated ≈ 21 A to match the load demand.
- **Stability:** Crucially, the DCM oscillations vanish instantly upon loading, as the high current forces the inductor into **Continuous Conduction Mode (CCM)**, resulting in a smooth steady-state operation.

3.3.4 Ripple Verification

Figure 5 confirms the design requirement. The zoomed-in waveform shows a triangular current ripple with a period of $100 \mu\text{s}$ (10 kHz), superimposed on the 300 Hz grid ripple caused by the rectifier.

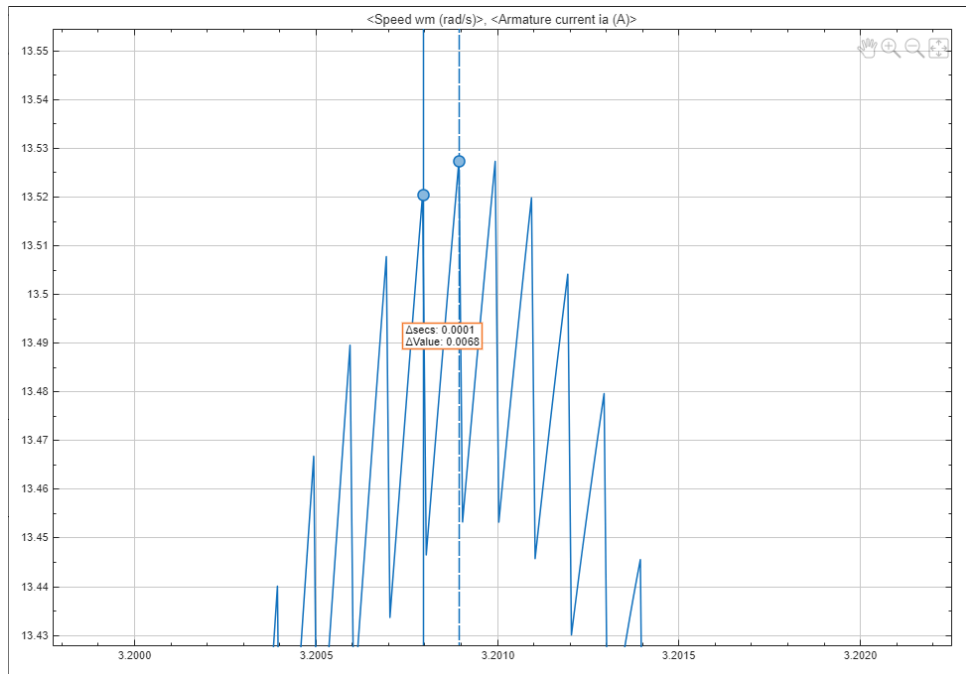


Figure 5: Armature Current Ripple Analysis. The simulation confirms $f_{sw} = 10$ kHz.

4 Component Selection and Sizing

The selection of power stage components was driven by the stress data obtained from the Phase II high-fidelity simulation and subsequent thermal analysis. Table ?? summarizes the key components selected for the hardware implementation.

4.1 Power Semiconductor Selection

4.1.1 Primary Switch (IGBT)

The simulation indicates a peak current of 25 A and a steady-state load of 21 A at 205 V.

- **Selected Component:** IXGH24N60C4D1 (600 V, 30 A).
- **Voltage Rating:** The 600 V rating provides a safety margin of nearly $3\times$ the DC link voltage, protecting against inductive voltage spikes.
- **Current Rating:** While the 30 A rating covers the load, the datasheet indicates this limit degrades rapidly with temperature. Detailed thermal calculations (Section 4.2) dictate the cooling solution.

4.1.2 Freewheeling Diode

The freewheeling diode carries the full load current during the "OFF" period of the duty cycle ($1 - D$).

- **Constraint:** A standard rectifier diode is too slow for 10 kHz switching, leading to shoot-through. An Ultrafast recovery diode ($t_{rr} < 60$ ns) is required.
- **Selected Component:** 2x MUR1560G connected in **Parallel**.
- **Justification:** A single MUR1560 is rated for only 15 A. Since the motor draws 21 A, a single diode would overheat and fail. Paralleling two devices doubles the thermal capacity and current handling to ≈ 30 A, ensuring safe operation.

4.1.3 Input Rectifier

- **Selected Component:** SQL3510 (3-Phase Bridge Module, 35 A / 1000 V).
- **Justification:** A dedicated three-phase bridge module was selected over discrete diodes to minimize wiring inductance and improve mechanical robustness against the grid inrush currents.

4.2 Thermal Management Design

A critical design finding was the high power dissipation in the semiconductor switches. Based on the datasheet parameters ($V_{CE(sat)} \approx 2.2$ V, $V_F \approx 1.4$ V):

$$P_{loss,total} \approx P_{IGBT} + P_{Diode} \approx (2.2 \text{ V} \times 21 \text{ A} \times D) + (1.4 \text{ V} \times 21 \text{ A} \times (1 - D)) \approx 50.5 \text{ W} \quad (6)$$

To maintain the junction temperature below 110°C in a 40°C ambient environment, the required thermal resistance is:

$$R_{\theta SA} \leq \frac{T_{J,max} - T_{amb}}{P_{loss}} = \frac{110 - 40}{50.5} \approx 1.38 \text{ °C/W} \quad (7)$$

Selection: The standard inventory TO-220 clip-on heatsinks ($R_{\theta} \approx 15 \text{ °C/W}$) are insufficient and would result in catastrophic failure. A **Large Extruded Aluminum Profile** (100 mm × 150 mm) or a forced-air CPU cooler is selected to achieve the required $< 1.38 \text{ °C/W}$ performance.

4.3 Gate Drive and Control Topology

Since the Buck Converter switch is referenced to the floating emitter node rather than ground, a high-side isolated driver topology is implemented.

- **Isolation:** **TLP250** Optocoupler. This provides galvanic isolation between the control logic and the high-voltage bus, while supplying the high peak currents required to charge the IGBT gate capacitance quickly ($< 200 \text{ ns}$).
- **Floating Supply:** **ROE-0512S** DC-DC Converter. This component converts the 5 V control logic power into a floating 12 V source dedicated solely to the TLP250 output stage, eliminating the need for bootstrap capacitors which can be unstable at variable duty cycles.
- **Controller:** An **Arduino** microcontroller is selected to generate the PWM. This choice allows for the precise software implementation of the 2-second Soft Start ramp, which is difficult to tune accurately with analog timers like the NE555.

4.4 Passive Components

- **DC Link Capacitor:** **2x 470 μF / 400 V** (Electrolytic). The inventory capacitors (63 V) were rejected due to the 210 V bus voltage. Two 400 V capacitors will be used to ensure sufficient voltage headroom and ripple current rating.
- **Protection:** A **25 A Fuse** is included on the AC input side to protect the variac and grid connection in the event of a semiconductor short circuit.

A Technical Note: Power Stage Semiconductor Selection

A.1 Executive Summary

Based on the high-fidelity simulation results and the available inventory list, this document evaluates the feasibility of using MOSFETs versus IGBTs for the main switching element.

Conclusion: The IRF740 MOSFET is technically unsuitable for this application due to insufficient current rating (10 A rating vs. 21 A demand) and excessive conduction losses (> 120 W). The **IXGH24N60C4D1 IGBT** is the only viable option in the inventory that meets the electrical and thermal safety margins.

A.2 System Requirements

According to the Phase II Simulation results, the power stage must meet the following criteria:

- **Steady-State Load Current (I_{load}):** 21 A
- **Peak Start-up Current:** 25 A
- **DC Link Voltage (V_{DC}):** Nominally 200 V (via Variac), with potential surges up to 540 V (3-Phase Rectified Peak).

A.3 Component Analysis: Option A (MOSFET)

Component: IRF740 N-Channel MOSFET

Ratings: $V_{DS} = 400V$, $I_D = 10A$, $R_{DS(on)} = 0.55\Omega$

A.3.1 Current Rating Violation

The motor requires a continuous current of 21 A. The IRF740 is rated for only 10 A at 25°C. Even if two MOSFETs are connected in parallel, the theoretical total capacity is 20 A. This is still below the continuous requirement (21 A) and significantly below the peak requirement (25 A).

A.3.2 Thermal Analysis (Power Loss)

MOSFET conduction loss is calculated as:

$$P_{cond} = I^2 \times R_{DS(on)} \quad (8)$$

Assuming a "Best Case" scenario with two parallel MOSFETs perfectly sharing current (effective $R_{DS(on)} = 0.275\Omega$):

$$P_{loss} = (21A)^2 \times 0.275\Omega \approx 121W \quad (9)$$

Result: Dissipating 121 W of heat from TO-220 packages is practically impossible without active liquid cooling.

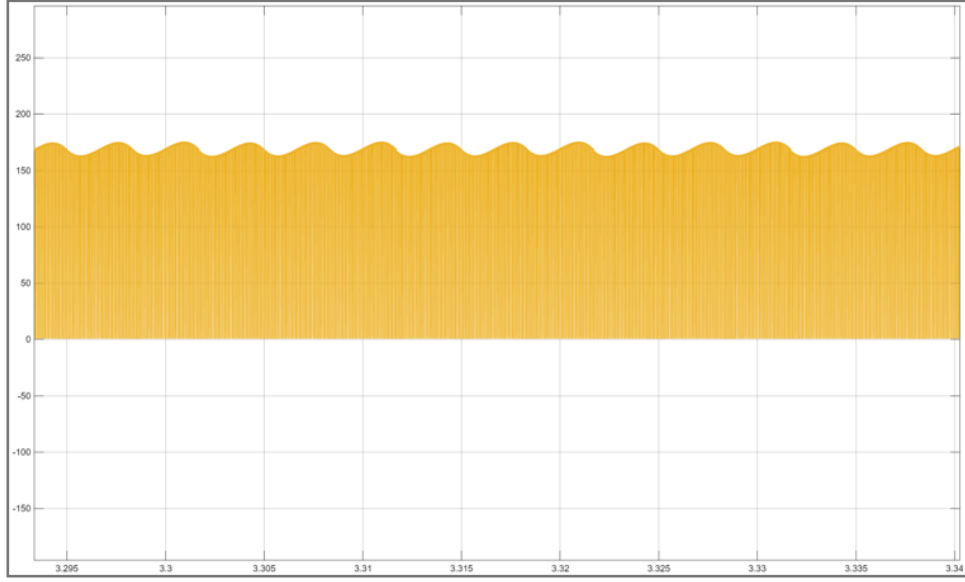


Figure 6: Steady-state dissipated MOSFET power vs. time.

A.4 Component Analysis: Option B (IGBT)

Component: IXGH24N60C4D1 IGBT

Ratings: $V_{CES} = 600V$, $I_C = 30A$, $V_{CE(sat)} \approx 2.2V$

A.4.1 Suitability and Thermal Analysis

The 30 A rating covers the demand. The conduction loss is approximated by:

$$P_{cond} \approx 2.2V \times 21A = 46.2 \text{ W} \quad (10)$$

This is less than 40% of the heat generated by the MOSFET solution.

A.5 Implementation Details

[Image of circuit implementation or gate driver schematic]

A.5.1 Gate Drive Strategy

Since the switch is on the high-side, we will utilize the **TLP250 Optocoupler** to provide galvanic isolation and a floating supply via the **ROE-0512S** DC-DC converter.

A.5.2 Final Recommendation

Use of parallel IRF740 MOSFETs presents an unacceptable risk. The **IXGH24N60C4D1 IGBT** is the mandatory choice.